Statistical Analysis of the 70 Meter Antenna Surface Distortions

K. Kiedron, C. T. Chian, and K. L. Chuang
Ground Antennas and Facilities Engineering Section

Statistical analysis of surface distortions of the 70 meter NASA/JPL antenna, located at Goldstone, was performed. The purpose of this analysis is to verify whether deviations due to gravity loading can be treated as quasi-random variables with normal distribution. Histograms of the RF pathlength error distribution for several antenna elevation positions have been generated. The results indicated that deviations from the ideal antenna surface are not normally distributed. The observed density distribution for all antenna elevation angles is taller and narrower than the normal density, which results in large positive values of kurtosis and a significant amount of skewness. The skewness of the distribution changes from positive to negative as the antenna elevation changes from zenith to horizon.

I. Introduction

The surface of the main reflector of a Cassegrain antenna is supposed to be a perfect paraboloid. In practice, however, there are systematic and random causes of surface irregularities. Ripples on the antenna surface as shown in Fig. 1 are basically a product of all gravity, wind and thermal loading effects. Additionally, some distortions are introduced at the factory during panel manufacturing, and some are caused by imperfect panel alignment and setting.

The gain loss, ΔG, due to reflector surface imperfections can be computed in decibels from:

$$\Delta G = 10 \log_{10} \eta \tag{1}$$

where the efficiency η is approximated by Ruze's (Ref. 1) equation as:

$$\eta = \exp -\left(\frac{4\pi\, rms}{\lambda}\right)^2 \tag{2}$$

where the root mean square (*rms*) of surface deviations is defined as one-half the change in the RF pathlength and λ is the operating wavelength (Refs. 2, 3). Fig. 2 illustrates the geometrical relationship, between an arbitrary surface displacement d, normal deviation n, and the corresponding RF pathlength deviation δ.

Ruze's Eq. (2) is derived under the assumption that the surface deviations δ_i at any surface point i are random variables having a Gaussian distribution with a zero mean and a standard deviation equal to the *rms* of the surface deviations of the reflector ($\delta_i \epsilon N(0, rms)$). Eqs. (1) and (2) are commonly used to estimate antenna gain loss even when surface distortions are due to deterministic causes such as gravity.

The purpose of this article is to verify whether deviations due to gravity can be treated as quasi-random variable with normal distribution. In order to eliminate truly random deviations (due to panel misalignment, wind turbulence and local thermal effects as well as measurement uncertainty) surface deviations simulated by a mathematical finite element model of antenna structure are used.

II. Data Description

The pathlength errors δ_i, due to gravity loading, measured from the least square best fit paraboloid were obtained for the 70 meter antenna from a finite element model generated with the JPL-IDEAS structural program. Five different antenna elevation positions, 0, 30, 60, 75 and 90 degrees, have been analyzed. Rigging position, that is 45 degrees, is excluded from analysis, because *rms* is zero at that elevation. Due to antenna symmetry, only one half of the dish, represented by $N = 715$ points, was modeled. The *rms* (root mean square) is calculated as:

$$rms = \sqrt{\sum_{i=1}^{N} \delta_i^2 \, \omega_i} \tag{3}$$

where N is the number of surface points and surface weighting factors w_i are proportional to the point tributary areas. The surface weighting factors w_i are normalized to meet the condition:

$$\sum_{i=1}^{N} w_i = 1 \tag{4}$$

Statistical analysis is performed on a new rescaled variable:

$$X_i = \delta_i \, \alpha_i \tag{5}$$

where

$$\alpha_i = \sqrt{w_i N}$$

Such a scaling allows direct comparison of the standard deviation of X and *rms*. The mean of X is approximately equal to zero (in all cases it was less than 0.013 mm) and the standard deviation agrees with the *rms* with better than 1% accuracy.

III. Test of Normality

For each antenna elevation position, a histogram of relative frequency distribution has been generated ($K = 30$ classes in -1.5 to 1.5 millimeter interval). Relative frequencies (probabilities in $\Delta x = 0.1$ millimeter segments) are obtained by division of each class frequency by the total number of points $N = 715$. The mean, m, and standard deviation, σ, for the particular elevation position have been calculated. Histograms with the normal counterparts $N(m, \sigma)$ are shown on Figs. 3, 4, 5, 6 and 7 for the elevation angles 0, 30, 60, 75, and 90 degrees respectively. In all five cases, histograms do not follow the normal distribution. The departure from normality is verified by computing the value of chi square χ^2 statistics according to the expression:

$$\chi^2 = N \sum_{i=1}^{K} \frac{(p_i - P_i)^2}{P_i} \tag{6}$$

where K is the number of classes, p_i is the probability of occurence of observed data in the i-th interval $(x_i, x_i + \Delta x)$ and P_i is the probability obtained from a hypothetical normal distribution $N(m, \sigma)$:

$$P_i = \frac{1}{\sqrt{2\pi}\,\sigma} \int_{x_i}^{x_i+\Delta x} \exp[-(x-m)^2/2\sigma^2] \, dx \tag{7}$$

The hypothesis that the observed distribution is normal can be rejected with probability higher than 0.99 due to the large values of χ^2/N (see Table 1). The same results can be obtained by using GFIT program from IMSL (International Mathematical and Statistical Library) which computes the goodness of fit by χ^2 statistics, but it uses equiprobable categories (Ref. 4).

Since it is possible that the estimate of m and σ are incorrect it was checked whether values of χ^2 statistics can be decreased for other normal distributions with different m and σ. Actually χ^2 was minimized with respect to m and σ. This resulted in finding a normal distribution which best fits the observed data. The results, after the best fit, are presented in Table 2. Again it can be concluded that with probability higher than 0.98, hypothesis of normality, must be rejected.

IV. Non-Normality Characterization

Since it was verified that gravity induced path length error is not normal for any antenna elevation position it is desirable to characterize the observed type of non-normality (Ref. 5). The two, skewness and kurtosis, parameters characterize the type of non-normality. Using higher moments about the mean: (with $k > 1$)

$$m_k = \frac{1}{N} \sum_{i=1}^{N} (X_i - m)^k, \qquad k = 2, 3, 4 \tag{8}$$

The coefficient of skewness is estimated according to the formula:

$$g_1 = \frac{m_3}{(m_2)^{3/2}} \tag{9}$$

where m_2 and m_3 are the second and third moments, respectively. If the sample comes from the normal population g_1 is approximately normally distributed with mean zero and standard deviation equal $\sqrt{6/N}$. The skewness measures the amount of symmetry around the mean. If low values of X are bunched close to the mean but high values extend far above the mean, this measure will be positive, since the large positive contributions of $(X-m)^3$, when X exceeds m, will predominate over the smaller negative contributions of $(X-m)^3$ obtained when X is less than m. In the population with negative skewness, the lower tail is the extended one, shifted to the left. In the population with positive skewness, the upper tail is the extended one, shifted to the right. The results of skewness for all elevation positions are shown in Table 3. The largest negative skewness is confirmed for the antenna at the horizon. Skewness decreases when the antenna approaches the rigging position (45 degrees). The largest positive skewness occurs for 60 degrees elevation and it decreases when the antenna approaches zenith position. The same trend can be observed on the histograms of Figs. 3, 4, 5, 6, and 7.

The degree of flattening of a probability density function near its mean is measured by the coefficient of kurtosis computed according to:

$$g_2 = \left(\frac{m_4}{m_2^2}\right) - 3 \tag{10}$$

In large samples, g_2 is normally distributed with mean zero and standard deviation equal $\sqrt{24/N}$. Positive values indicate that the probability density function is more sharply peaked, that is taller and narrower, than the normal density. Flat-topped distributions show negative kurtosis. The kurtosis parameter for all antenna elevation positions is presented in Table 3. Since the sample's values of g_2 are much larger than the standard error $\sqrt{24/N}$, the positive kurtosis parameter is confirmed for every antenna elevation position. Again, this result of exceeding the normal peak is noticeable on the histograms of Figs. 3, 4, 5, 6, and 7.

V. Summary

The statistical analysis of the 70 meter antenna surface distortions indicated that deviations from ideal paraboloid are not normally distributed. The distribution for all elevation angles is taller and narrower than normal density, which results in large positive values of the kurtosis and a significant amount of skewness. The skewness of the distribution changes from negative to positive as the antenna elevation angle changes from horizon to zenith. Therefore, the gravity induced deformations violate the assumption of normality in Ruze's equation. It is reasonable, however, to assume that for small departures from normality Ruze's equation will provide a good estimate of antenna gain loss. Nevertheless, the following open problem is posed: what modifications, if any, should be applied to Ruze's equation to incorporate non-zero skewness and kurtosis as a function of antenna elevation positions? Therefore Ruze's formula should be verified for non-normal quasi-random distribution by comparing it with results produced by the exact expression for antenna efficiency in the theory of electromagnetic scattering and diffraction (Ref. 6).

Acknowledgment

The authors gratefully acknowledge stimulating discussions with JPL colleagues Dr. F. Lansing, Dr. R. Levy and M. S. Katow.

References

1. Ruze, J., "The Effect of Aperture Errors on the Antenna Radiation Pattern," *Nuevo Cimento Suppl.*, Vol. 9, No. 3, pp. 364–380, 1952.

2. Utku, S., and Barondess, S. M., "Computation of Weighted Root-Mean-Square of Path Length Changes by the Deformations and Imperfections of Rotational Parabolidal Antennas," *JPL Technical Memorandum 33-118*, Jet Propulsion Laboratory, Pasadena, Calif., March 1963.

3. Kiedron, K., "Homology Deviation Measure for Microwave Antenna Design," *IEEE Montech '86 Conference on Antennas and Communications*, Montreal Canada, pp. 173–176, September 1986.

4. Kendall, M. G., and Stuart, A., "*The Advanced Theory of Statistics*," Vol. 2, Hafner Publishing Company, New York, 1961.

5. Snedecor, G. W., and Cochran, W. G., "*Statistical Methods*" Sixth Edition, The Iowa State University Press, Ames, Iowa, 1967.

6. Rahmat-Samii, Y., "An Efficient Computational Method for Characterizing the Effects of Random Surface Errors on the Average Power Pattern of Reflectors," *IEEE Transactions Antennas and Propagation, AP-31*, No. 1, January 1983.

Table 1. Chi square goodness of fit test: m and σ one obtained with standard estimators

Elevation angle	m	σ	χ^2/N
0	-0.013	0.646	0.188
30	-0.003	0.204	0.600
60	0.002	0.190	0.239
75	0.002	0.367	0.183
90	0.001	0.534	0.090

Table 2. Chi square goodness of fit test: m and σ minimize x^2

Elevation angle	m	σ	χ^2/N
0	0.059	0.576	0.145
30	-0.013	0.239	0.233
60	0.008	0.215	0.156
75	-0.010	0.407	0.134
90	-0.003	0.474	0.069

Table 3. Skewness and kurtosis test

Elevation angle	Skewness	Kurtosis
0	-1.338	2.77
30	-0.972	1.82
60	0.568	1.61
75	0.429	2.16
90	0.363	2.99
$\sqrt{6/N}$	0.092	
$\sqrt{24/N}$		0.183

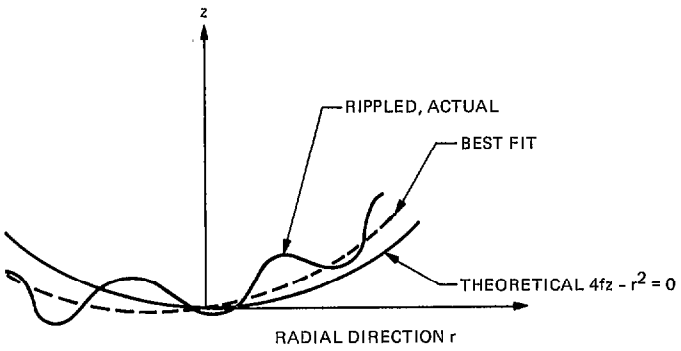

Fig. 1. Surface of main reflector

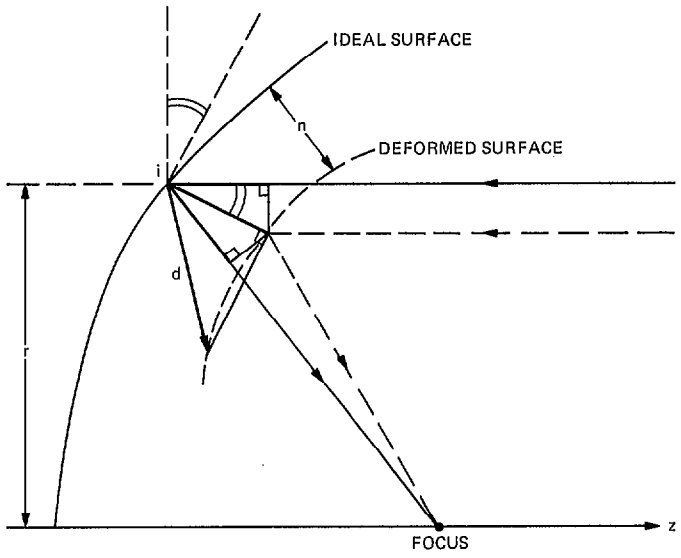

Fig. 2. Geometrical relationship between surface displacement *d*, normal deviation *n*, and corresponding *RF* pathlength deviation σ

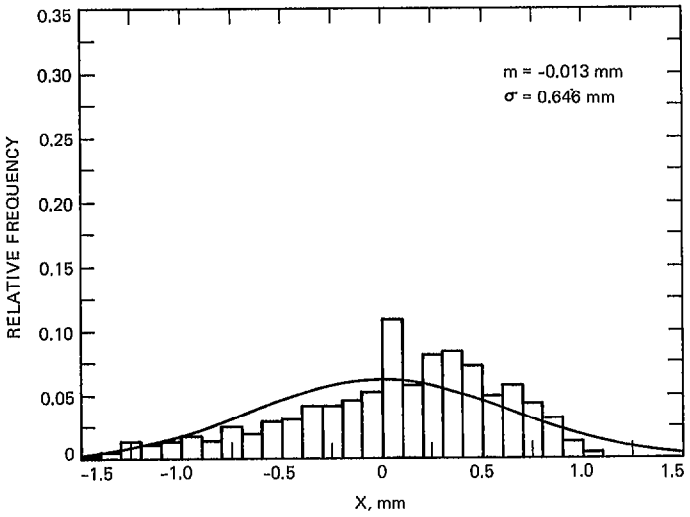

Fig. 3. Histogram of *RF* pathlength error distribution at 0 degree elevation

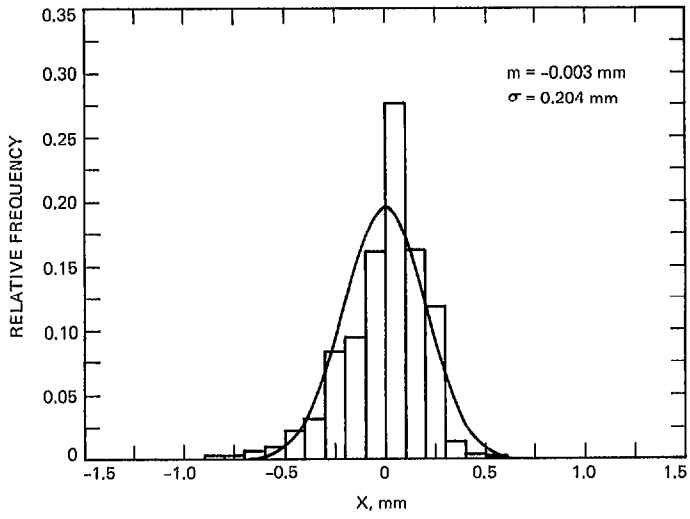

Fig. 4. Histogram of *RF* pathlength error distribution at 30 degree elevation

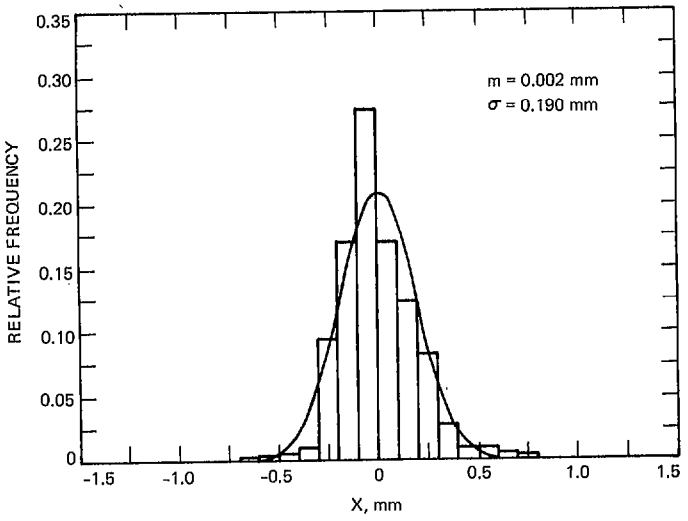

Fig. 5. Histogram of *RF* pathlength error distribution at 60 degree elevation

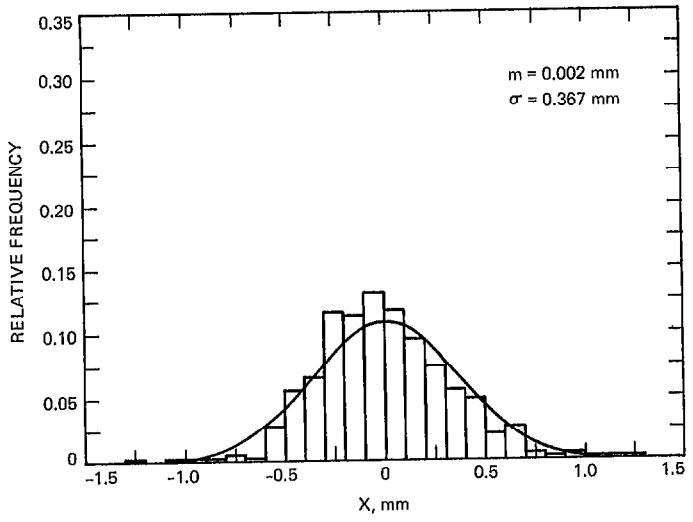

Fig. 6. Histogram of *RF* pathlength error distribution at 75 degree elevation

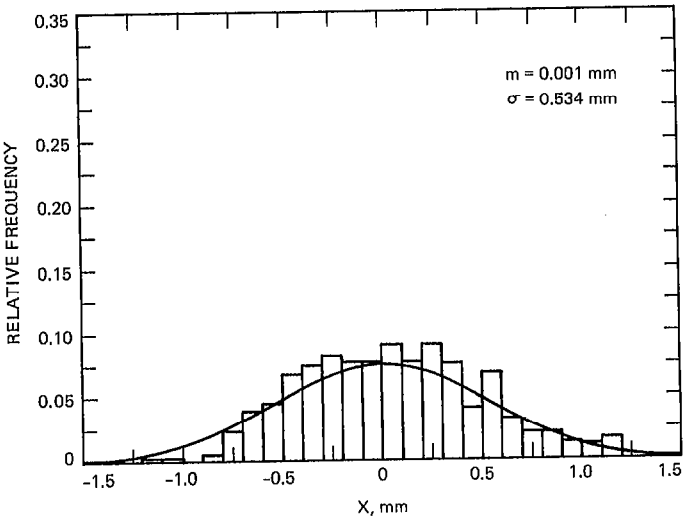

Fig. 7. Histogram of *RF* pathlength error distribution at 90 degree elevation